

Topological phase and lattice structures in spin chain models

Yan-Chao Li,¹ Jing Zhang,¹ and Hai-Qing Lin²

¹ College of Materials Science and Opto-Electronic Technology,
University of Chinese Academy of Sciences, Beijing, China

² Beijing Computational Science Research Center, Beijing, China

(Dated: March 12, 2022)

Finding new topological materials and understanding the physical essence of topology are crucial problems for researchers. We study the topological property based on several proposed Su-Schrieffer-Heeger (SSH) related models. We show that the topologically non-trivial phase (TNP) in the SSH model can exist in other model conditions and can even be caused by anisotropy; its origin has a close relation with the even-bond dimerization. Further study shows that the TNP is not determined by the periodicity of the system, but the parity of the two kinds of bonds plays a significant role for the formation of the TNP. This finding reveals the topological invariant of the system and might supply potential extended topological materials for both theoretical and experimental researches.

PACS numbers: 05.30.Rt, 03.67.-a

I. INTRODUCTION

Topological phases, with their remarkable properties, have been intensively studied in recent years^{1,2}. Many novel quantum phenomena or quantum physical matters, such as the quantum Hall effect, topological insulators, and topological superconductors, are related to topological phases. A prominent feature of a topological phase is the topologically protected edge states, which are robust against the specific edge shape and impurity perturbations and could be useful for applications ranging from spintronics to quantum computations^{1,3}.

In contrast to conventional phases of matter which are characterized by symmetry properties and local order parameters, topological phases are not determined by a specific state, such as the ground state, but are related to the whole energy spectrum of the system. They do not belong to the framework of Landau's symmetry breaking theory and cannot thereby be characterized by local order parameters⁴⁻⁶. Therefore, most studies on topological matters only focus on their novel phenomena or how to detect or characterize topological phases using edge states or topological invariants^{3,7}. Few works study their formation causes and influence factors that are significant for a comprehensive understand of a topological phase. This issue in strongly correlated quantum systems still remains as a challenge.

In addition, the realization of lattice models using ultra-cold gases and superconducting quantum circuits has attracted great attention in recent years⁸⁻¹¹. Spin chains can be experimentally simulated through neutral atoms or polar molecules stored in an optical lattice¹²⁻¹⁵, trapped ions¹⁶⁻¹⁹, and NMR simulator²⁰. As the trapped molecules as an example, the trapped molecules have two internal states (the lowest rovibrational state and an excited rotational state) and can be used to modify a spin-1/2 degree of freedom. Via a microwave field, the molecules can be coupled and the dipolar interaction will induce spin exchanges between pairs of molecules. Recently, in the presence of an external dc electric field, a

spin XXZ model was realized experimentally, and the spin-spin interactions can be tuned with the external electric field or modified by choosing different pairs of rotational levels¹⁴.

The topological phenomena could also emerge in the synthetic systems, such as the cold atoms in optical lattices and qubits in superconducting quantum circuits^{10,21-27}. Moreover, as these artificial spin lattices could be applied local interaction change by a local external field modulation, they could thereby serves as a nature platform for the study of relation between topology and structure. In addition, spin-based devices have their advantages because of the absence of scattering due to conduction electrons. A zero-temperature spin transport has been studied in a finite spin-1/2 XXZ chain coupled to fermionic leads with a spin bias voltage²⁸. For such devices defects and impurity cannot be neglect and will play quite important roles in the quantum-state property including the topologically non-trivial phase (TNP) and its applications. Therefore, in this paper we study a series of related spin chain models to reveal the relation of the topological quantum phase and different symmetric interactions structures.

II. MODEL AND METHODS

The Hamiltonian of the Su-Schrieffer-Heeger (SSH) related XXZ spin model can be written as follows:

$$H = - \sum_{j=1}^N [(1 + \eta) (\sigma_{2j-1}^x \sigma_{2j}^x + \sigma_{2j-1}^y \sigma_{2j}^y + \Delta_1 \sigma_{2j-1}^z \sigma_{2j}^z) + (1 - \eta) (\sigma_{2j}^x \sigma_{2j+1}^x + \sigma_{2j}^y \sigma_{2j+1}^y + \Delta_2 \sigma_{2j}^z \sigma_{2j+1}^z)], \quad (1)$$

where N is the total number of spins, η denotes the dimerization at even or odd bonds (for convenience, we denote the $1 - \eta$ interacted bonds as B^- and denote those $1 + \eta$ interacted bonds as B^+), Δ_m ($m = 1, 2$) describe

the anisotropy of the system arising from the spin-spin interaction on the XY plane and the Z coordinate direction and can be different for odd and even bonds, and σ^α ($\alpha = x, y, z$) are the Pauli matrices.

When $\Delta_1 = \Delta_2 = \Delta = 0$ and set $\sigma^x = \sigma^+ + \sigma^-$ and $\sigma^y = i(\sigma^+ - \sigma^-)$, Eq. (1) becomes to the spin SSH-XX model. Its Hamiltonian can be written as follows:

$$H = - \sum_{j=1}^N 2[(1+\eta)(\sigma_{2j-1}^+ \sigma_{2j}^- + \sigma_{2j-1}^- \sigma_{2j}^+) + (1-\eta)(\sigma_{2j}^+ \sigma_{2j+1}^- + \sigma_{2j}^- \sigma_{2j+1}^+)], \quad (2)$$

this Hamiltonian is soluble and its quantum phase transitions (QPTs) have been studied from the thermodynamics point of view²⁹. Actually, it has an analogous expression and a same position of critical point (CP) with the spinless SSH model^{30,31}. However, the σ operators here are spin operators and satisfy commutate relation, while the operators in the Hamiltonian of the spinless SSH model are fermion operators and satisfy anti-commutate relation for the spinless model. They actually describe different physical nature.

To study the topology, one feasible method is to find topological invariants, in which the Berry phase has been successfully used as a detector to reveals the topological nature of the system^{32,33}. Under the twisted boundary conditions, a phase of ϕ is imposed in the boundary conditions, and the range of phase values 2π is discretized into M points, i.e., $\phi_1, \phi_2, \dots, \phi_M$. Then the Berry phase is defined as

$$\gamma = -i \sum_{l=1}^M \ln U(\phi_l) \quad (3)$$

where $U(\phi_l) = \psi^*(\phi_l)\psi(\phi_{l+1})$ is the link variable³¹. In the topological region the Berry phase is π and in the topological trivial phase it vanishes.

In addition, the entanglement entropy $(E_v)^{34-36}$ and the maximum of quantum coherence QC_{\max}^{37} has been successfully used to detect different QPTs, therefore, the quantum phase transitions of the systems are also studied by these two detectors. The detector QC_{\max} is defined as follows

$$QC_{\max} = \max I(\rho_{ab}, K_{\sigma_n}) = \max -\frac{1}{4} \text{Tr}[\rho_{ab}, K_{\sigma_n}]^2. \quad (4)$$

where [...] denotes the commutator, ρ_{ab} is the reduced density matrix for two nearest-neighbour sites a and b , and the K_{σ_n} is written as $K_a \otimes I_b$ ³⁸, in which the Pauli matrices σ_n with an arbitrary direction \vec{n} is an observable at site a :

$$\sigma_n = \begin{pmatrix} \cos \theta & \sin \theta e^{-i\varphi} \\ \sin \theta e^{i\varphi} & -\cos \theta \end{pmatrix}, \quad (5)$$

the maximum is taken by traversing θ and φ from 0 to 2π . In addition, given a known reduced density matrix ρ_{ab} , the von Neumann entropy $E_v(\rho_{ab}) = -\text{Tr} \rho_{ab} \ln \rho_{ab}$ ³⁵.

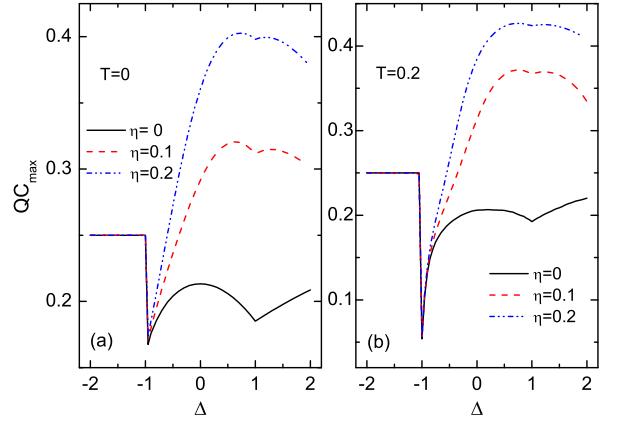


FIG. 1: (Color online) QC_{\max} under different η from (a) ED method for $N = 16$ and (b) TMRG method at $T = 0.2$.

To calculate the Berry phase and the detectors, we use the exact diagonalization (ED) techniques as well as the transfer-matrix renormalization-group technique (TMRG). The TMRG method is based on a Trotter-Suzuki decomposition of the partition function of a system, which maps a d -dimensional quantum system to a $d+1$ -dimensional classical one; therefore it can directly handle infinite spin chains for an overview, see Ref 39. For accuracy, we take $m=200$ states for the TMRG calculations. The Trotter-Suzuki error is less than 1×10^{-3} and the truncation error is smaller than 1×10^{-8} .

III. QPTS AND TOPOLOGICALLY NON-TRIVIAL PHASE IN THE SPIN SSH-LIKE SYSTEMS

A. Alternated interaction bonds in the spin SSH-XXZ model

We first study the topological phase and QPTs in the SSH-XXZ model. When $\eta = 0$ and $\Delta_1 = \Delta_2 = \Delta$, Eq. (1) describes the XXZ spin model. There are two CPs: a continuous phase transition at $\Delta = 1$ and a first-order transition at $\Delta = -1$ ⁴⁰. When $\Delta > 1$ it is the antiferromagnetic (AF) phase with a Néel order $\langle \sigma_j^z \rangle = -\langle \sigma_{j+1}^z \rangle$, it is the critical Tomonaga-Luttinger liquid (TLL) phase between $-1 < \Delta < 1$, and it is the fully polarized phase at $\Delta < -1$ ⁴¹. The QC_{\max} results using ED method for $N = 16$ are shown in Fig. 1(a). The CPs are clearly identified by the two turning points at $\Delta = \pm 1$, which is consistent with the results in Ref. 42. When η is added, the two CPs still exist and always keep their positions unchanged. In other words, the dimerized parameter η does not change the critical phenomena of the XXZ model. To eliminate the finite-size effect we modulate the infinite-size case using TMRG numerical algorithm. The results further confirm the ED results as shown in Fig. 1(b).

Figure 2(a) gives a complete exhibition of the critical

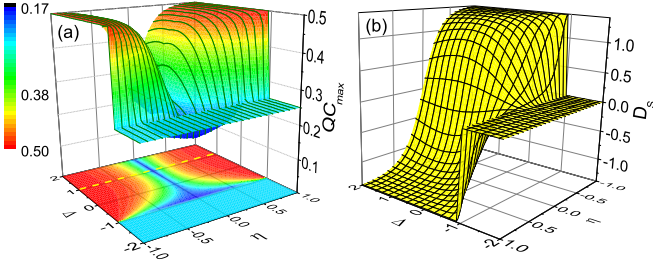


FIG. 2: (Color online) (a) QC_{\max} and its contour map and (b) the dimerization D_s as functions of Δ and η for $N = 8$. The dashed line in (a) indicates the breaking point of QC_{\max} .

regions. The CPs at $\Delta = \pm 1$, which segment the system into the AF, TLL, and polarized phases, extend to the whole $-1 < \eta < 1$ region, and there appears a segment at $\eta = 0$ for $\Delta > -1$. Through spin arrangement analysis and the unified structure of QC_{\max} , we conclude that η does not destroy the AF, TLL, and polarized orders, but it will introduce the dimerized property. Figure 2(b) shows the dimerization D_s defined as follows³⁶:

$$D_s = E_{\text{even}} - E_{\text{odd}} \quad (6)$$

where E_{odd} and E_{even} are the neighboring two-site entropies connected by odd and even bonds in the chain, respectively. One can see that except the $\Delta < -1$ region and the $\eta = 0$ line, D_s is not zero in the whole parameter regions. The nonzero D_s confirms the dimerized orders in these regions. Given the sign of D_s , we conclude that, for the AF and TLL phases, i.e., $\Delta > -1$ region in Fig. 2(a), there are two kinds of dimerized phases separated by $\eta = 0$ line: it is the even-bond dimerized structure for $\eta > 0$, while it is the odd-bond dimerized state for $\eta < 0$. The polarized phase is not influenced by η , it extends to the whole $\Delta < -1$ region.

To further study the topological property, we calculate the twisted boundary Berry phase as shown in Fig. 3. The topological nontrivial phase at $\eta < 0$ for the spin SSH model extends to a wide parameter region (see the π value in the whole $\Delta > -1$ region) with its CP at $\eta = 0$ unchanged. Compared to the dimerized property D_s in Fig. 2(b), the topologically non-trivial phase is consistent with the even-bond dimerized regions. This could be understood as follows: the topological phase are actually caused by the competed dimerizations between odd and even bonds. Compared to the spin SSH model, Δ term only introduces anisotropy to the SSH-XXZ model, it does not change the dimerized structure of the SSH model, therefore, except of the polarized phase which has no dimerized factors, the topological property also does not change with Δ .

B. Different dimerized term on the Z direction

To further reveal the relations between dimerization and TNP and the Z-Z interaction effects, we consider

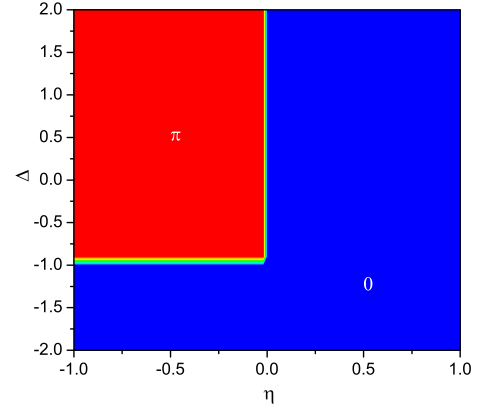


FIG. 3: (Color online) Contour map of the Berry phase as functions of Δ and η under twisted boundary conditions. The red color π -value region corresponds to the topologically non-trivial phase while the blue color 0-value region indicates the topologically trivial phase.

$\Delta_1 \neq \Delta_2$ in Eq. refeq:1, which correspond to the dimerization rate on the Z direction different from that of the XY plane.

For simplify, we consider $\delta_1 = 0$ and $\delta_2 = 0$ cases, respectively. The Berry phase results are shown in Fig. 4(a). The π value region that indicates the topological nontrivial phase is quite different with that of the SSH-XXZ model. When $\Delta_2 = 0$, the system is the spin SSH model, the CP is at $\eta = 0$. As δ_2 increases, the interaction along Z direction has a same sign as that of X and Y direction. Thus, it will enlarge the even-bond dimerization. The regime of the topological nontrivial phase is then enlarged. When $\delta_2 < 0$, the sign of interaction along Z direction is opposite with that of X and Y direction. It will weaken the antiferromagnetic effect along the XY direction and will weaken the even-bond dimerized trends. The results are consistent with this point, the topological nontrivial phase becomes narrow and narrow and disappears at the critical point at $\Delta_2 = -1$, where the system is polarized along the Z direction. The dimerization D_s in Fig 4(b) further confirms the conclusion. The positive region that corresponds the even dimerized states consist with the topological nontrivial phase region in Fig 4(a).

Just as Δ_2 affect the even-bond dimerized condition, Δ_1 has a similar effect but on the odd bonds. Thus, it has an opposite effect for the formation of the even-bond dimerization. The results are shown in Fig. 4(c). As Δ_1 change from positive to negative the region of topological nontrivial phase is enlarged continuously, which indeed has an opposite effect with Δ_2 . Now we can conclude that the interaction on the Z direction affects the dimerization of odd and even bonds, and thereby affects the TNP; The TNP mainly comes from the competition of the odd and even bond interactions, or more precisely, the even-bond dimerization plays an important role for the formation of the TNP.

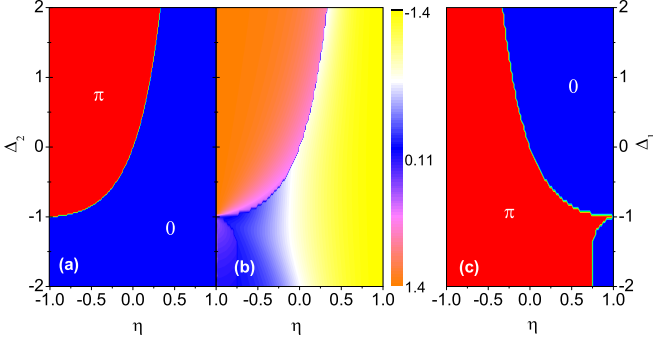


FIG. 4: (Color online) Contour map of the twisted boundary Berry phase as functions of (a) Δ_2 and η at $\Delta_1 = 0$ and (c) Δ_1 and η at $\Delta_2 = 0$ for $N = 8$; (b) the dimerization D_s at the same condition as (a).

C. Topologically non-trivial phase and anisotropy

The above results show that the topologically non-trivial phase is mainly caused by the alternated different interactions along the spin chain. We now consider a uniform interaction between neighboring bonds but with a different anisotropy conditions between odd and even bonds. The Hamiltonian is given by

$$H = - \sum_j [(1 + \beta_1) (\sigma_{2j-1}^x \sigma_{2j}^x + \sigma_{2j-1}^y \sigma_{2j}^y) + (1 + \beta_2) (\sigma_{2j}^x \sigma_{2j+1}^x + \sigma_{2j}^y \sigma_{2j+1}^y)] + [(1 - \beta_1) (\sigma_{2j-1}^z \sigma_{2j}^z) + (1 - \beta_2) (\sigma_{2j}^z \sigma_{2j+1}^z)], \quad (7)$$

where β_1 and β_2 describe the anisotropy between Z and XY directions on odd and even bonds, respectively, the operator $c_{j,\alpha}$ has the same meaning as in Eq. (1).

The Berry phase contour map results are shown in Fig. 5. Taking the $\beta_1 = \beta_2$ line as the phase boundary, the system exhibits the topological nontrivial phase (indicated by the π value in the red region) as long as $\beta_2 > \beta_1$. This condition corresponds to a larger even-bond interaction on the XY direction. Considering the preceding conclusion that the even-bond dimerized state is responsible for the formation of the TNP, we conclude now that the interactions along XY direction is more dominant than that on the Z direction for the formation of TNP. In addition, the Berry phase for larger system, such as $N=24$, shows a same result. Therefore, the TNP is indeed exist in this anisotropy case but not caused by the finite-size effects.

IV. TOPOLOGICALLY NON-TRIVIAL PHASE AND LATTICE STRUCTURE

The above results are all related to the difference of interaction conditions on odd and even bonds, or more precisely the different interactions between odd and even bonds on the XY direction leads to the TNP. Then there

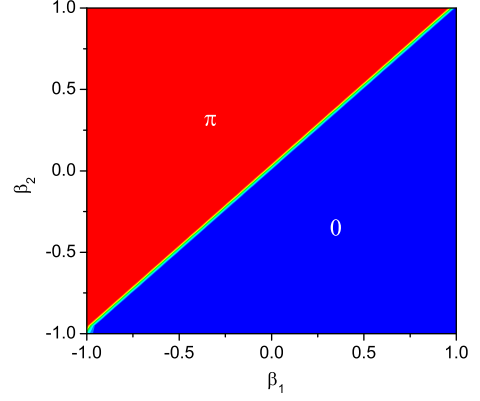


FIG. 5: (Color online) The contour map of twisted boundary Berry phase as functions of β_1 and β_2 for the anisotropy case at $N = 8$.

is an elementary question whether the different alternated odd and even bonds is a necessary condition for the formation of the TNP. To answer this question we turn to study the relationship between the TNP and interactional structures in the spin chain.

On the other hand, when impurities are considered, the periodically alternated odd and even bonds structure in the SSH-XXZ model would be destroyed, and there would be introduced the kinks to the chain⁴³. This condition should be more realistic in nature. Moreover, the recently developed artificial quantum systems, such as ultra-cold atom in optical lattices, trapped ions, and superconducting quantum circuits, makes it possible to provide tunable and flexible experimental manipulations. Therefore, we propose an blocks (marked as ellipse and rectangle, respectively) alternated structure to describe and simulate the random arrangement of the two kinds of interactional bonds (B^+ and B^-).

This is sketched in Fig. 6(a), where the ellipses and rectangles circles those continuous arranged B^- and B^+ bonds with coupling constant $1 - \eta$ and $1 + \eta$, respectively; the bond quantities in the m -th ellipse and the m -th rectangle are written as E_m and R_m , respectively (for random, the values of E_m can be different for different m , and R_m has a same condition); the lowercase letters represents different spins and N is the system size. The Halmiltonian can be written as follows:

$$H = H_E + H_R$$

$$H_E = - \sum_{j=1}^{M_E} (1 - \eta) (\sigma_{j_l}^x \sigma_{j_r}^x + \sigma_{j_l}^y \sigma_{j_r}^y)$$

$$H_R = - \sum_{j=1}^{M_R} (1 + \eta) (\sigma_{j_l}^x \sigma_{j_r}^x + \sigma_{j_l}^y \sigma_{j_r}^y), \quad (8)$$

where H_E and H_R describe the terms connected by $1 - \eta$ and $1 + \eta$ with a total corresponding bond numbers M_E and M_R , respectively, and j_l and j_r are the left and right spin sites connected by the j -th bond, respectively.

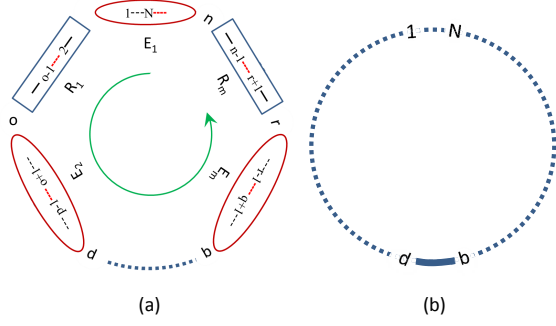


FIG. 6: (Color online) Schematic sketch of the random arrangement of two kinds of interactional bonds. (a) The ellipses and rectangles circles those continuous arranged B^- and B^+ bonds with coupling constant $1 - \eta$ and $1 + \eta$, respectively [the black lines in the ellipses (dashed) and rectangles (solid) correspond to the B^- and B^+ bonds, respectively and the red dashed lines represent the omitted same bonds in the same block]; the bond number in the m -th ellipse and the m -th rectangle are noted as E_m and R_m , respectively (to reflect the randomness, the values of E_m can be different for different m . R_m has the same condition); each lowercase letter represent an arbitrary spin and the green circular curve with arrow indicates the increasing direction of the spin arrangement. (b) a limited case with only one B^- bond between spins p and q while the left bonds are all B^+ bonds.

When each elliptic block and each rectangular block contain only one bond, the Hamiltonian describes the spin SSH model as in Eq. (1) at $\Delta_1 = \Delta_2 = 0$. It becomes the spin XX model with a defect when there is only one rectangle with one B^- bond while the other bonds are all the B^+ bonds as sketched in Fig. 6(b). The number of the ellipses and rectangles and the bond number they contained (given by the values of E_1 to E_m and R_1 to R_m , respectively) determine the bond structure of the system. We consider a simplest case first, namely, the SSH-XX bond structure but with some B^- bonds replacing by B^+ bonds. When the number of the replaced bonds is noted as K , the Berry phase as a function of η under different K for an $N = 20$ chain are plotted in Fig. 7(a). The π value Berry phase, which indicates the TNP, always exists in the $\eta < 0$ region under different K -value cases. This property is consistent with that of the SSH-XX model. It seems that the changes of bond structures does not influence the topological property of the system. Because the periodicity here has been damaged in these $K \neq 0$ cases, the topological property thereby can not be connected with it. Looking into the structure of these different cases, there is only one common property: the number of the two kind bonds (B^+ and B^-) at each ellipse and rectangle are odd. This feature may play a decisive role for the TNP. To further understand the natural origin of the topology, we turn to the parity of the two kinds of bonds in each ellipse and rectangle.

We consider various possible odd-numbered B^+ and B^- bonds alternated cases and find they show the same

Berry phase feature. Figure 7(b) shows the results of three cases of them. The π Berry phase at $\eta < 0$ region is completely consistent with the results in Fig. 7(a). The TNP indicated by the π Berry phase is robust to the bond configurations: as long as the number of both the B^+ and B^- bonds in a continuous block keeps odd, no matter what the number is. The limiting case sketched in Fig. 7(b) satisfies the odd-numbered bonds condition. Thus, it also hold the same topological property. Figure 7(c) shows the results under different system size N . The Berry phase curve does not change as N increases. This feature eliminates the finite-size effects and confirms the already anticipated topological property. As the replaced B^+ bonds can be regarded as kinks caused by defects or impurities or can be treated as the local manipulations in an artificial quantum simulator such as ultra-cold lattice, this finding points out a class of systems that may have important potential applications on topology research.

For comparison, we then study the other cases with different bond parity. The Berry phase results for even-numbered B^+ and B^- bonds alternated cases are shown in Fig. 7(b) as the lines without symbol. One can see that the Berry phase always equals zero in all the parameter region. There is no any sign of the TNP. Afterwards, we further calculate the cases with both odd- and even- numbered bond blocks at the same time. Although the results show that there could appear the π Berry phase indicated topological state, the critical points corresponding to the nontrivial to trivial do not stay at $\eta = 0$ any more. Therefore, we conclude that the topological non-trivial phase in the spin SSH-like systems comes from the odd-numbered

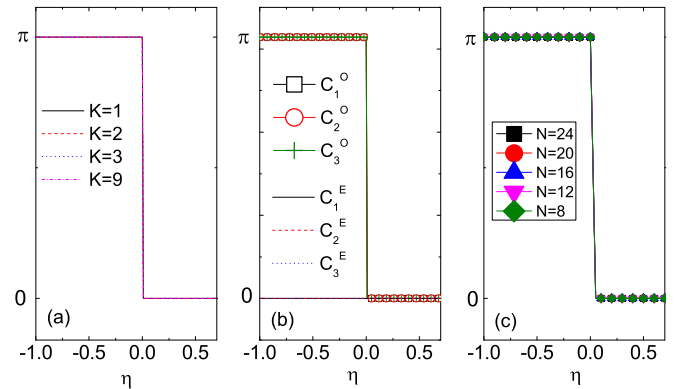


FIG. 7: (Color online) Berry phase results for different spin structures (a) the SSH model with K B^+ bonds replaced by B^- bonds (b) the line and symbol cures are for B^+ and B^- bonds alternated cases: $R_1 = R_2 = 5, E_1 = 1, E_2 = 9$ for C_1^O , $R_1 = R_2 = 7, E_1 = E_2 = 3$ for case C_2^O , and $R_1 = R_2 = 3, R_3 = 7, E_1 = E_2 = 1, E_3 = 5$ for case C_3^O ; the lines without symbol are for the even B^+ and B^- bonds alternated cases: $R_1 = R_2 = 8, E_1 = E_2 = 2$ for C_1^E , $E_1 = R_1 = E_2 = E_3 = E_4 = R_4 = 2$ and $R_3 = R_5 = 4$ for C_2^E , $E_1 = \dots = E_5 = P_1 = \dots = P_5 = 2$ for C_3^E ; (c) only $R_1 = 1$ the left bonds are all circled by E_1 under different N .

alignment of the two kinds of bonds.

V. SUMMARY

In summary, we study the topological property of a class of one-dimensional spin chains based on several SSH-XXZ related models by Berry phase and several detectors of QPTs. We consider the TNP in the spin SSH-XXZ-like model first. Combined with the results of quantum coherence, entanglement entropy, and Berry phase, we conclude that the TNP can exist in a wide parameter range, and it has a quite close relation with the even-bond dimerized state. We then consider the aspect of anisotropy and found that the TNP can also appear in an anisotropic system.

To further reveal the physical essence of topology, we study the relation between the TNP and interactional-bond structures. The periodicity and parity of the bond arrangements in the chain are mainly focused. The results show that the TNP is not determined by the periodicity of the interaction bonds in the system, it can

exist under several kinds of aperiodic cases. On the other hand, the parity of the two kinds of bonds in their own continuous arranged part plays a significant role for the formation of TNP. The system keeps the same topological property as long as it possesses an odd-odd alternated block arrangement for the two kinds of bonds, no matter how many blocks it consists and how many bonds are there in each block, while its topological property will change under other cases. This finding reveals the topological invariant of the system and might supply extended topological materials or states by doping in solid state context or local modulation in quantum-simulator systems.

Acknowledgments

We acknowledge supports from NSAF U1530401, National Natural Science Foundation of China under Grant No. 11104009 and computational resources from the Beijing Computational Science Research Center.

-
- ¹ M. Z. Hasan and C. L. Kane, Rev. Mod. Phys. **82**, 3045 (2010).
 - ² X.-L. Qi and S.-C. Zhang, Rev. Mod. Phys. **83**, 1057 (2011).
 - ³ X. Zhan, L. Xiao, Z. H. Bian, K. K. Wang, X. Z. Qiu, B. C. Sanders, W. Yi, and P. Xue, Phys. Rev. Lett. **119**, 130501 (2017).
 - ⁴ X. Y. Feng, G. M. Zhang, and T. Xiang, Phys. Rev. Lett. **98**, 087204 (2007).
 - ⁵ X. G. Wen, *Quantum Field Theory of Many-body Systems*, (Oxford University, New York, 2004).
 - ⁶ S. Sachdev, *Quantum Phase Transitions*, (Cambridge University Press, Cambridge, UK, 2000).
 - ⁷ X. P. Wang, L. Xiao, X. Z. Qiu, K. K. Wang, W. Yi, and P. Xue, Phys. Rev. A **98**, 013835 (2018).
 - ⁸ E. Zohar, J. I. Cirac, and B. Reznik, Rep. Prog. Phys. **79**, 014401 (2016).
 - ⁹ M. Dalmonte and S. Montangero, Contemp. Phys. **57**, 388 (2016).
 - ¹⁰ X. S. Tan, D. W. Zhang, Q. Liu, G. M. Xue, H. F. Yu, Y. Q. Zhu, H. Yan, S. L. Zhu, and Y. Yu, Phys. Rev. Lett. **120**, 130503 (2018).
 - ¹¹ J. Wiese, Nucl. Phys. **A931**, 246 (2014).
 - ¹² J. Simon, W. S. Bakr, R. Ma, M. Eric Tai, P. M. Preiss, and M. Greiner, Nature (London) **472**, 307 (2011).
 - ¹³ B. Yan, S. A. Moses, B. Gadway, J. P. Covey, K. R. A. Hazzard, A. M. Rey, D. S. Jin, and J. Ye, Nature (London) **501**, 521 (2013).
 - ¹⁴ K. R. A. Hazzard, B. Gadway, M. Foss-Feig, B. Yan, S. A. Moses, J. P. Covey, N. Y. Yao, M. D. Lukin, J. Ye, D. S. Jin, and A. M. Rey, Phys. Rev. Lett. **113**, 195302 (2014).
 - ¹⁵ J. Struck, C. Ölschläger, R. Le Targat, P. Soltan-Panahi, A. Eckardt, M. Lewenstein, P. Windpassinger, and K. Sengstock, Science **333**, 996 (2011).
 - ¹⁶ D. Porras and J. I. Cirac, Phys. Rev. Lett. **92**, 207901 (2004).
 - ¹⁷ K. Kim, M. S. Chang, R. Islam, S. Korenblit, L. M. Duan, and C. Monroe, Phys. Rev. Lett. **103**, 120502 (2009).
 - ¹⁸ K. Kim, M. S. Chang, S. Korenblit, R. Islam, E. E. Edwards, J. K. Freericks, G. D. Lin, L. M. Duan, and C. Monroe, Nature (London) **465**, 590 (2010).
 - ¹⁹ R. Islam, E. E. Edwards, K. Kim, S. Korenblit, C. Noh, H. Carmichael, G. D. Lin, L. M. Duan, C. C. Joseph Wang, J. K. Freericks, and C. Monroe, Nat. Commun. **2**, 377 (2011).
 - ²⁰ Z. K. Li, H. Zhou, C. Y. Ju, H. W. Chen, W. Q. Zheng, D. W. Lu, X. Rong, C. K. Duan, X. H. Peng, and J. F. Du, Phys. Rev. Lett. **112**, 220501 (2014).
 - ²¹ M. Atala, M. Aidelsburger, J. T. Barreiro, D. Abanin, T. Kitagawa, E. Demler, and I. Bloch, Nat. Phys. **9**, 795 (2013).
 - ²² G. Jotzu, M. Messer, R. Desbuquois, M. Lebrat, T. Uehlinger, D. Greif, and T. Esslinger, Nature (London) **515**, 237 (2014).
 - ²³ M. Aidelsburger, M. Lohse, C. Schweizer, M. Atala, J. T. Barreiro, S. Nascimbene, N. R. Cooper, I. Bloch, and N. Goldman, Nat. Phys. **11**, 162 (2015).
 - ²⁴ N. Flächner, B. S. Rem, M. Tarnowski, D. Vogel, D.-S. Lühmann, K. Sengstock, and C. Weitenberg, Science **352**, 1091 (2016).
 - ²⁵ T. Li, L. Duca, M. Reitter, F. Grusdt, E. Demler, M. Endres, M. Schleier-Smith, I. Bloch, and U. Schneider, Science **352**, 1094 (2016).
 - ²⁶ M. Leder, C. Grossert, L. Sitta, M. Genske, A. Rosch, and M. Weitz, Nat. Commun. **7**, 13112 (2016).
 - ²⁷ E. J. Meier, F. A. An, and B. Gadway, Nat. Commun. **7**, 13986 (2016).
 - ²⁸ F. Lange, S. Ejima, T. Shirakawa, S. Yunoki, and H. Fehske, Phys. Rev. B **97**, 245124 (2018).
 - ²⁹ J. H. H. Perk, H. W. Capel, M. J. Zuilhof, Th. J. Siskens,

- Physica A **81**, 319 (1975); J. H. H. Perk, arXiv:1710.03384.
- ³⁰ R. Wakatsuki, M. Ezawa, Y. Tanaka, and N. Nagaosa, Phys. Rev. B **90**, 014505 (2014).
- ³¹ W. C. Yu, Y. C. Li, P. D. Sacramento, and H. Q. Lin, Phys. Rev. B **94**, 245123 (2016).
- ³² H. Guo and S.Q. Shen, Phys. Rev. B **84**, 195107 (2011).
- ³³ H. Guo, S.Q. Shen and S. Feng, Phys. Rev. B **86**, 085124 (2012).
- ³⁴ A. Osterloh, L. Amico, G. Falci, and R. Fazio, Nature **416**, 608 (2002).
- ³⁵ S. J. Gu, S. S. Deng, Y. Q. Li, and H. Q. Lin, Phys. Rev. Lett. **93**, 086402 (2004).
- ³⁶ Ö. Legeza, and J. Sólyom, Phys. Rev. Lett. **96**, 116401 (2006).
- ³⁷ Y. C. Li and H. Q. Lin, Unpublished.
- ³⁸ E. P. Wigner, M. M. Yanase, Proc. Natl. Acad. Sci. USA **49**, 910 (1963).
- ³⁹ T. Xiang and X. Wang, in Density-Matrix Renormalization: A New Numerical Method in Physics, edited by I. Peschel, X. Wang, M. Kaulke, and K. Hallberg (Springer, New York, 1999), pp. 149C172; U. Schollwock, Rev. Mod. Phys. **77**, 259 (2005).
- ⁴⁰ M. Takahashi, Thermodynamics of One-dimensional Solvable Models (Cambridge University Press, Cambridge, England, 1999).
- ⁴¹ S. Takayoshi and M. Sato, Phys. Rev. B **82**, 214420 (2010).
- ⁴² T. Werlang, C. Trippé, G. A. P. Ribeiro, and G. Rigolin, Phys. Rev. Lett. **105**, 095702 (2010).
- ⁴³ L. Yu, Solitons and Polarons in Conducting Polymers (World Scientific, Singapore 1988).